

LOW AND HIGH TEMPERATURE MICROMECHANICAL BEHAVIOR OF BN/3003 ALUMINUM ALLOY NANOCOMPOSITES

A. CHENNAKEESAVA REDDY

Professor, Department of Mechanical Engineering, JNT University, Hyderabad, India

ABSTRACT

The aluminum 3003 alloy is used in manufacturing of cooking utensils, pressure vessels, ice cube trays, refrigerator panels, heat exchangers, etc. In recent years, hexagonal boron nitride has been focused as a filler material for the metal matrix composites used for low or high temperature applications. Micromechanical properties were analyzed for the BN/3003 Al alloy nanocomposites using ANSYS software code. The major conclusion of the present work is that the interphase between BN nanoparticle and 3003 Al alloy has been found to be the weakest zone either low or high temperature operating conditions.

KEYWORDS: 3003 Al Alloy, Low or High Temperature, Hexagonal Boron Nitride, Micromechanics

INTRODUCTION

The 3003 aluminum (Al) alloy with a major alloying element of manganese (1.0 to 1.5%) is used in manufacturing of cooking utensils, pressure vessels, ice cube trays, refrigerator panels, heat exchangers, etc. This alloy has medium strength but exhibits good resistance to atmospheric corrosion. Also, this alloy has good weldability and cold formability. This alloy is not heat treatable and develops strengthening from cold forming only. Alternatively, the strength and stiffness of lightweight 3003 Al alloy can be enhanced by reinforcing with ceramic nanoparticles. Variety of Al alloys were reinforced with different ceramic nanoparticles such as SiC [1, 2], Al₂O₃ [3, 4], AlN [5, 6], ZrO₂ [7], B₄C [8, 9], Fe₃O₄ [10], Fe₂O₃ [11], Si₃N₄ [12, 13], MgO [14, 15], TiO₂ [16], TiN [17], TiC [18, 19], SiO₂ [20, 21], and TiB₂ [22].

In recent years, hexagonal boron nitride (BN) has drawn a lot of attraction in the field of metal matrix composites. It offers very high thermal conductivity and good thermal shock resistance. It is anisotropic in its mechanical properties due to the platy hexagonal crystals and their orientation. The objective of this work was, to estimate thermal shock resistance of BN/3003 Al alloy metal matrix composites subjected to cryogenic and high temperature conditions. The micromechanical properties were analyzed using ANSYS software code.

MATERIALS AND METHODS

In the present work, matrix and reinforcement materials were, respectively, 3003 aluminum (Al) alloy and hexagonal boron nitride. For the micromechanical analysis, the representative volume element (RVE) model of hexagonal array was assumed for the BN nanoparticles distributed in the 3003 Al alloy metal matrix. The size and shape of BN nanoparticles were average diameter of 80 nm and hexagonal as shown in Figure 1. The volume fraction of BN nanoparticles was 10%. An interphase around the BN nanoparticle was also taken into account for the micromechanical analysis. The plane strain boundary conditions were imposed on hexagonal array RVE models for the numerical analysis. Prior to exercise finite element analysis, the 3003 Al alloy was tested for unidirectional tensile loading at low temperature

conditions of -100°C , -50°C , 0°C and at high temperature conditions of 100°C , 200°C , and 300°C . Two chambers were designed for testing at low and high temperatures. Low and high temperatures were, respectively, achieved by forced convection for heating and liquid nitrogen injection system for cooling. The RVE models were numerically tested for the ultimate tensile strength (assuming that first occurrence of fracture in the matrix) of the 3003 Al alloy at different temperatures. The results obtained from the finite element analysis were validated with experimentally tested samples of the BN/3003 Al alloy nanocomposites.

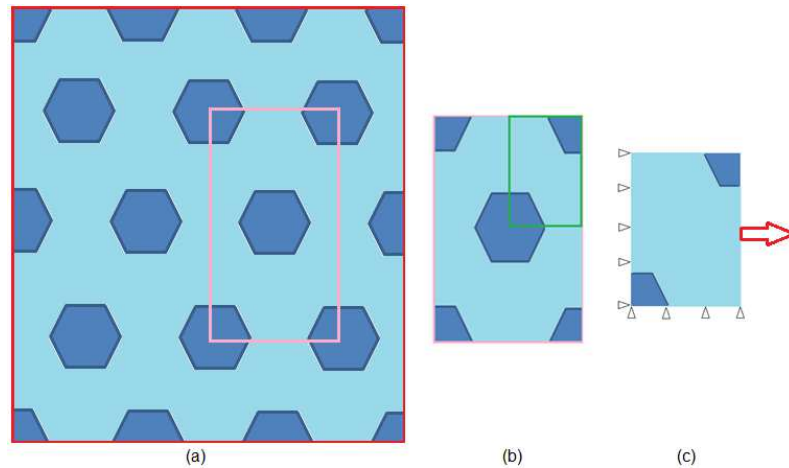


Figure 1: BN Nanoparticles in 3003 Al Alloy Matrix: (a) Random Distribution, (b) Hexagonal RVE and, (c) One-Fourth Model of Hexagonal RVE

RESULTS AND DISCUSSIONS

Because of symmetry, one-fourth of the model was used in the finite element analysis, as shown in Figure 2a. Solid 8-node 183 was used to discretize both the BN nanoparticle and 3003 Al alloy. Cohesive 8-node 205 was used for the interphase. The symmetry boundary conditions were applied the left-side and bottom of the one-fourth of model, as shown in Figure 2b. The loading of hexagonal RVE at different temperatures is shown in Figure 3. The tensile strength of 3003 Al alloy decreases with an increase in temperature applied to the tensile specimen at slow strain rate testing (SSRT) of 10^{-3} s^{-1} . The selection of the strain rate is very significant because the vulnerability to cracking may not be evident from the result of tests at too low or too high strain rate.

Displacement, as a function of applied temperature and pressure on the BN/3003 Al alloy composites is shown in Figure 3. The ultimate tensile strength was decreased with an increase of temperature for 3003 Al alloy as shown in Figure 3. For temperatures -50°C and -100°C , the resultant displacement (contraction due to applied temperature and elongation due to tensile loading) is negative representing the behavior of shrinkage. Even though the applied load is of tensile in nature, the contraction is dominated due to cryogenic effect. This shrinkage is very small for the BN nanoparticles, but much greater for the 3003 Al alloy. Further, the shrinkage is higher in the direction normal to the tensile loading than that in the direction parallel to the loading. Above 0°C , the resultant displacement (elongation due to applied temperature and tensile loading) increases very steeply with an increase in temperature. Here again, even if the applied tensile load is low, the elongation is dominated due to high temperature effect. The elongation is very small for the BN nanoparticles but much greater for the 3003 Al alloy. The contraction or elongation of the BN nanoparticles is very small on account of their high stiffness (100 MPa) as compared to that (69 MPa) of 3003 Al alloy. The raster images obtained from the finite element analysis confirm the same trend as that observed in Figure 3a.

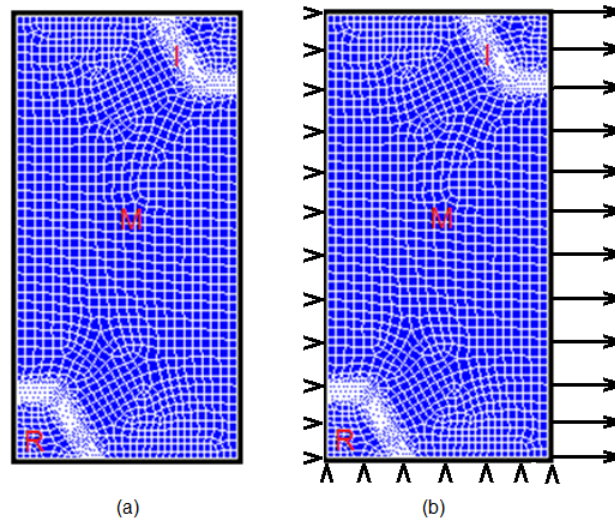


Figure 2: Finite Modeling of RVE Composed of Matrix (M) Reinforcement (R), and Interface (I): Discretization and (b) Boundary Conditions and Loading

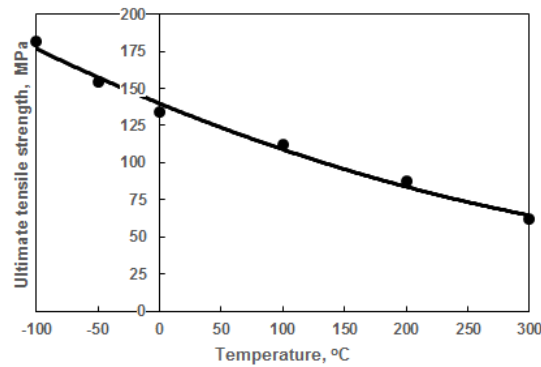


Figure 3: Effect of Temperature on Ultimate Tensile Strength of 3003 Al Alloy

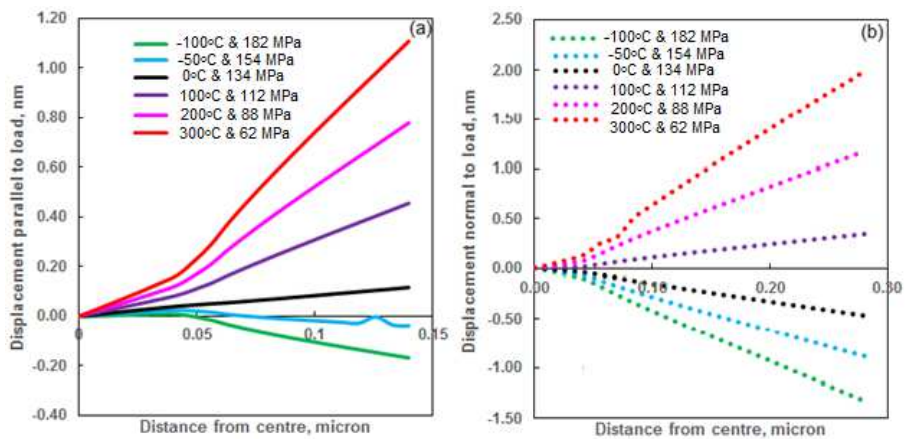


Figure 4: Effect of Temperature and Pressure on Displacement of BN/3003 Al Nanocomposites

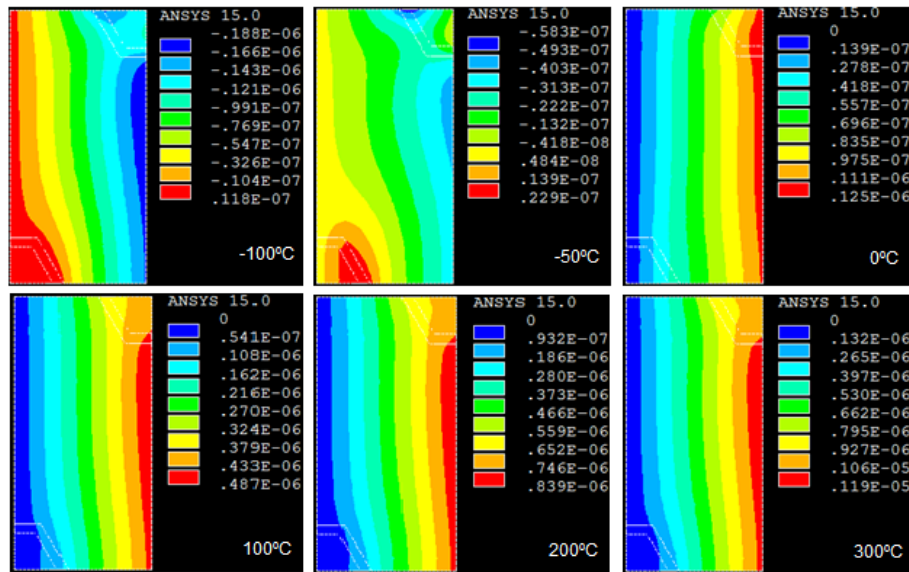


Figure 5: Raster Images of Displacements of BN/3003 Al Alloy Nanocomposite Parallel to Load Direction

As seen from Figure 5a, the tensile strain increases with an increase in the temperature. The interphase region between the BN nanoparticle, the 3003 and Al alloy matrix is also observed. Below 100°C and along normal to the load direction as seen from Figure 5b, the strains induced in the BN/3003 Al alloy nanocomposites are compressive owing to contraction/compression of BN nanoparticles and 3003 Al alloy. But, the induced strains normal to the load direction are tensile in nature above 200°C due to the domination of thermal expansion. The tensile stresses increase in the BN nanoparticle, while they decrease in the 3003 Al alloy with increase of temperature, as understood from Figure 6a. Below 0°C, the BN nanoparticle experiences compressive stresses in the direction normal to the applied load due to shrinkage, and it experiences tensile stresses due to thermal expansion above 0°C. The augmentation of stresses in the BN nanoparticle is the characteristic of effective load transfer from the matrix to the reinforcement.

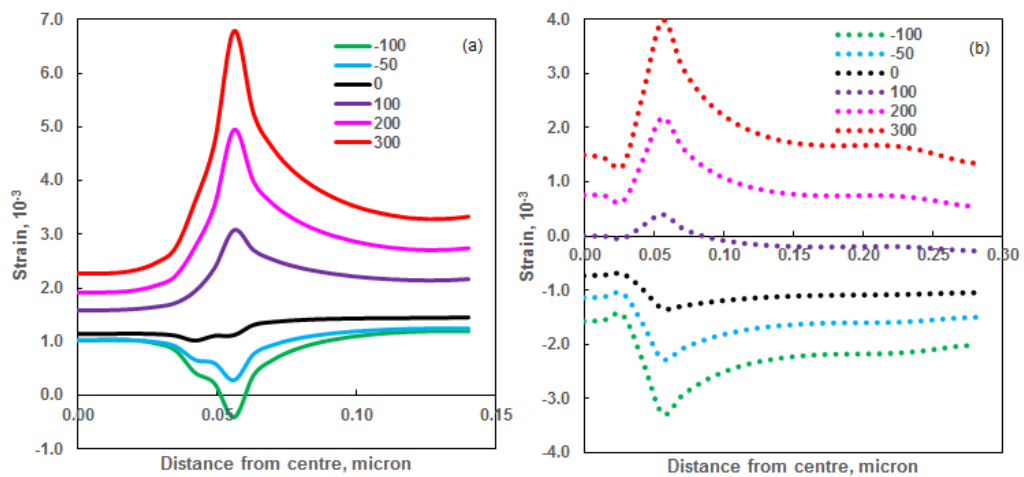


Figure 6: Effect of Temperature and Pressure on Strains of BN/3003 Al Nanocomposites

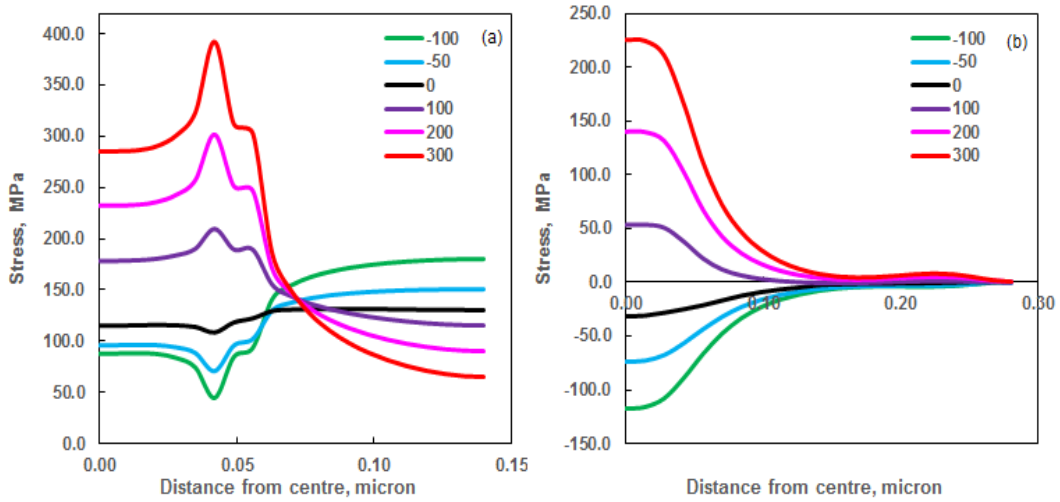


Figure 7: Effect of Temperature and Pressure on Stresses of BN/3003 Al Nanocomposites

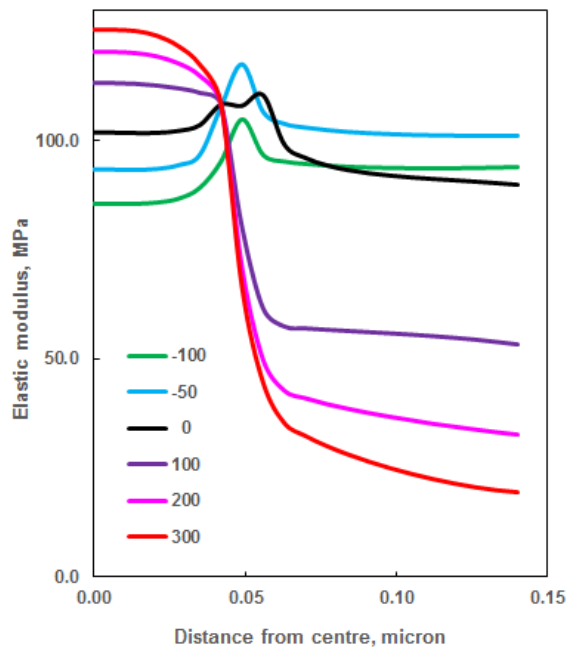


Figure 8: Effect of Temperature and Pressure on Elastic Modulus of BN/3003 Al Nanocomposites

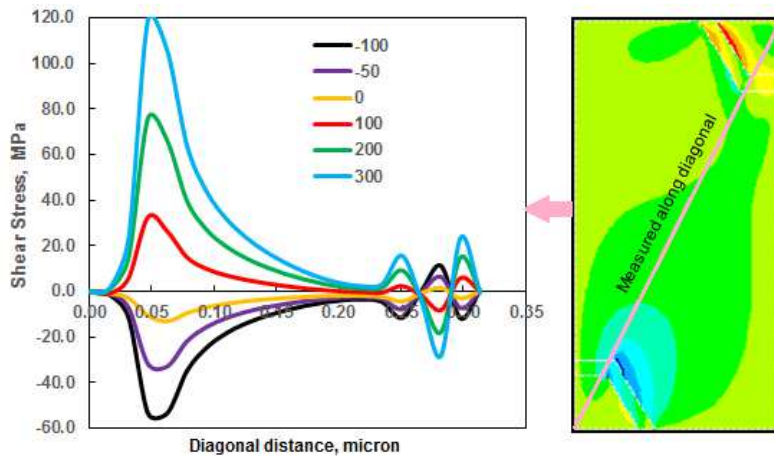


Figure 9: Effect of Temperature and Pressure on Shear Stress of BN/3003 Al Nanocomposites

As observed from Figure 7 that the elastic modulus of the matrix material decreases with increase from -100°C to 300°C , while the stiffness of BN nanoparticle increases with an increase in temperature. But, the interphase material has experienced high compressive shear stress below 0°C and high tensile shear stress above 0°C . Hence, the weakest zone seems to be the interphase region for the chance to pull out or decohesion as seen from Figure 8. The raster images reveal the same. At -100°C , the compressive shear stress is -105 MPa near the interphase region as illustrated in Figure 9. Again, at the interphase region, the tensile shear stress is 243 MPa as demonstrated in Figure 9. The scanning electron microscopy as revealed in Figure 10 proves the said phenomena near the interphase region, due to the high stress intensity developed, because of the pull out.

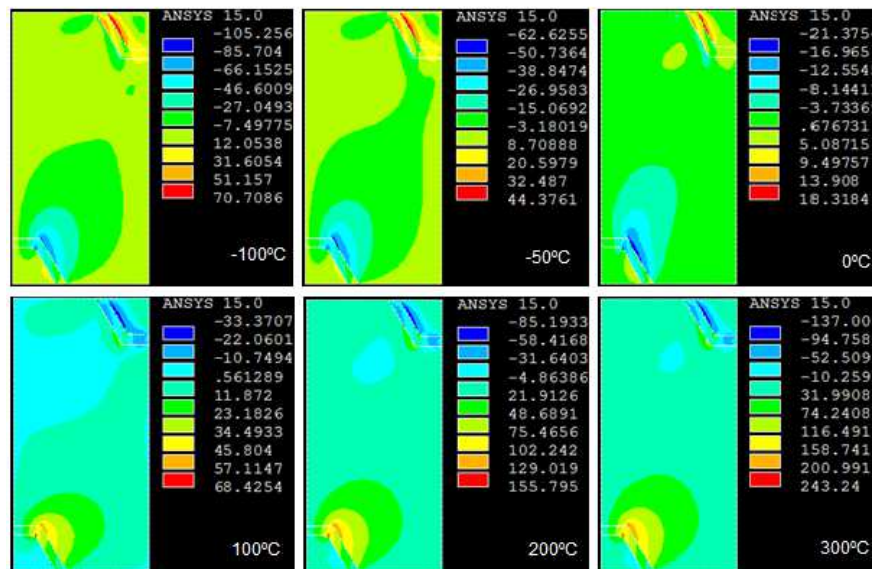


Figure 10: Raster Images of Shear Stresses Induced in BN/3003 Al Alloy Nanocomposites

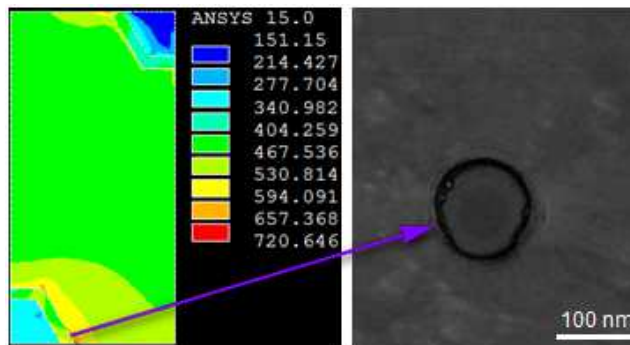


Figure 11: Fracture in BN/3003 Al Alloy Nanocomposite

CONCLUSIONS

The micromechanical analysis could illustrate the actual behavior of BN/3003 Al alloy nanocomposites at low and high temperature operating conditions. Neither BN nanoparticle nor 3003 Al alloy would fracture, but the interphase between them. The assumption of the hexagonal RVE array would be an appropriate choice for establishing the micromechanical behavior of BN/3003 Al alloy nanocomposites.

REFERENCES

1. P.M. Singh, J. J. Lewandowski, "Effects of heat treatment and reinforcement size on reinforcement fracture during tension testing of a SiCp discontinuously reinforced aluminum alloy," *Metallurgical and Materials Transactions A*, 24, pp. 2531–2543, 1993.
2. A. C. Reddy, "Evaluation of mechanical behavior of Al-alloy/SiC metal matrix composites with respect to their constituents using Taguchi techniques," *I-manager's Journal of Mechanical Engineering*, 1 (2), pp. 31-41, 2011.
3. P. Poza, J. Llorca, "Fracture Toughness and Fracture Mechanisms of Al-Al₂O₃ Composites at Cryogenic and Elevated Temperatures," *Materials Science and Engineering A*, 206, pp. 183-193, 1996,
4. A. C. Reddy, Essa Zitoun, "Tensile behavior of 6063/Al₂O₃ particulate metal matrix composites fabricated by investment casting process," *International Journal of Applied Engineering Research*, 1 (3), pp. 542-552, 2010.
5. M. N. Wahab, A. R. Daud, M. J. Ghazali, "Preparation and characterization of stir cast-aluminum nitride reinforced aluminum metal matrix composites, *International Journal of Mechanical and Materials Engineering*, 4 (2), pp. 115-117, 2009.
6. A. C. Reddy, "Necessity of Strain Hardening to Augment Load Bearing Capacity of AA1050/AlN Nanocomposites," *International Journal of Advanced Research*, 3 (6), pp. 1211-1219, 2015.
7. B. R. Alavala, "Micromechanics of Thermoelastic Behavior of AA6070 Alloy/Zirconium Oxide Nanoparticle Metal Matrix Composites," *International Journal of Engineering Research & Science*, 2 (2), pp. 1-8, 2016.
8. K. Kalaiselvan, N. Murugan, Siva Parameswaran, "Production and characterization of AA6061-B₄C stir cast composite," *Materials and Design*, 32, pp. 4004–4009, 2011.
9. C. R. Alavala, "Synthesis and Tribological Characterization of Cast AA1100-B₄C Composites," *International Journal of Science and Research*, 5 (6), pp. 2404-2407, 2016.
10. E. Bayraktar, D. Katundi, "Development of a new aluminium matrix composite reinforced with iron oxide (Fe₃O₄)," *Journal of Achievements in Materials and Manufacturing Engineering*, 38, pp. 7-14, 2010.
11. A. C. Reddy, "Reduction of Vibrations and Noise using AA7020/Fe₂O₃ Nanocomposite Gear Box in Lathe," *International Journal of Scientific & Engineering Research*, 6(9), pp. 685-691, 2015.
12. H. Wang, S. Wang, G. Liu, Y. Wang, "AlSi11/Si₃N₄ interpenetrating composites Tribology properties of aluminum matrix composites," *Advances in Materials Physics and Chemistry*, World Congress on Engineering and Technology, pp. 130-133, 2012.
13. C. R. Alavala, "Adhesive and Abrasive Wear Behavior of AA4015 Alloy/Si₃N₄ Metal Matrix Composites," *Indian Journal of Engineering*, 13 (34), pp. 625-633, 2016.
14. M.A. Baghchesara, H. Abdizadeh, H.R. Baharvandi, "Microstructure and Mechanical Properties of Aluminum Alloy Matrix Composite Reinforced with Nano MgO Particles," *Asian Journal of Chemistry*, 22 (9), pp. 6769-6777, 2010.

15. C. R. Alavala, "Thermal Expansion Behavior of Al/Magnesia Metal Matrix Composites," *International Journal of Science and Research*, 5 (8), pp. 1817-1821, 2016.
16. C. R. Alavala, "Tribological Investigation of the Effects of Particle Volume Fraction, Applied Load and Sliding Distance on AA4015/Titania Nanocomposites," *IPASJ International Journal of Mechanical Engineering*, 4 (10), pp. 9-15, 2016.
17. C. R. Alavala, "Effect of Thermoelastic Behavior on interfacial debonding and Particulate Fracture in AA1100/TiN Nanoparticulate Metal Matrix Composites," *International Journal of Science and Research*, 5 (3), pp. 1295-1300, 2016.
18. N. Samer, J. Andrieux, B. Gardiola, N. Karnatak, O. Martin, H. Kurita, L. Chaffron, S. Gourdet, S. Lay, O. Dezellus, "Microstructure and mechanical properties of an Al-TiC metal matrix composite obtained by reactive synthesis," *Composites Part A: Applied Science and Manufacturing*, 72, pp. 50 – 57, 2015.
19. C. R. Alavala, "Micromechanical Modelling of Thermoelastic Behavior of AA7020/TiC Metal Matrix Composites," *International Journal of Scientific, Engineering and Research*, 4 (2), pp. 1-5, 2016.
20. H. Zuhailawati, P. Samayamutthirian, C. H. M. Haizu, "Fabrication of low cost of aluminium matrix composite reinforced with silica sand," *Journal of Physical Science*, 18(1), pp. 47–55, 2007
21. C. R. Alavala, "Nano-mechanical modeling of the thermoelastic behavior of AA6061/silicon oxide nanoparticulate metal matrix composites," *International Journal of Science and Research*, 5 (1), pp. 550-553, 2016.
22. S. Kumar, M. Chakraborty, V. Subramanya Sarma, B.S. Murty, "Tensile and wear behaviour of in situ Al-7Si/TiB₂ particulate composites," *Wear*, 265, pp. 134–142, 2008.